Effect of thermostatic expansion valve tuning on the performance enhancement and environmental impact of a mobile air conditioning system

Rajendran Prabakaran[1] · Dhasan Mohan Lal[1] · Sukumar Devotta[2]

Abstract

In this work, the performance enhancement of a HFO-1234yf mobile air conditioning (MAC) system with a suction/liquid line heat exchanger (SLHX) was carried out experimentally by tuning the thermostatic (constant superheat) expansion valve (TXV) and its impact on the environment was also evaluated. The optimum charge of HFO-1234yf and HFC-134a systems was found to be 670 g and 740 g, respectively. The results showed that the HFO-1234yf system with SLHX had better coefficient of performance (COP) and exergy efficiency when compared to HFC-134a system with SLHX at idling condition, whereas it had reduced performance at other speed conditions. The tuning of the TXV in the HFO-1234yf system had a positive influence on the COP, cooling capacity, and exergy efficiency and those were higher than that of existing HFC-134a system by 4.3–8.6%, 6.5–10.1%, and 3.7–5.1%, respectively, at idling and city speed conditions, whereas those were slightly lower at high-speed conditions. The total CO_2 equivalent emission of tuned and un-tuned HFO-1234yf system was 27.98% and 24.64% lower than that of the existing HFC-134a system. The outcome of this study indicated that the SLHX implementation in the HFO-1234yf MAC system with tuned TXV could be a possible option to replace HFC-134a.

Keywords Global warming potential · HFO-1234yf · Total equivalent warming impact · Suction line heat exchanger · Thermostatic expansion valve · COP

Abbreviations

CC	Compressor volumetric capacity (m^3 min^{-1})
CFC	Chlorofluorocarbon
GWP	Global warming potential
HC	Hydrocarbon
HFC	Hydrofluorocarbon
HFO	Hydrofluoroolefin
HVAC	Heating, ventilation and air conditioning
IRD	Integrated receiver dryer
MAC	Mobile air conditioning
ODP	Ozone depleting potential
RPM	Revolution per minute
RPS	Regulated power supply
SLHX	Suction line heat exchanger
TEWI	Total equivalent warming impact
TFA	Trifluoroacetic acid
TXV	Thermostatic expansion valve
VCR	Vapour compression refrigeration
VFD	Variable frequency drive

Symbols

COP	Coefficient of performance
DBT	Dry bulb temperature (°C)
DSC	Degree of subcooling (°C)
DSH	Degree of superheating (°C)
$\dot{E}$	Exergy rate (kW)
ED	Exergy destruction rate (kW)
EDR	Exergy destruction ratio
h	Enthalpy (kJ kg^{-1})
L	Average refrigerant leakage (%)
$\dot{m}$	Mass flow rate (kg s^{-1})
M_f	Mass of fuel used (L)
M_s	Refrigerant charge quantity (g)
N	System lifetime (years)
P	Pressure (bar)
Q	Heat transfer (kW)

✉ Dhasan Mohan Lal
dr.mohanlal29@gmail.com

1   R&AC Division, Department of Mechanical Engineering, Anna University, Chennai, India

2   National Environmental Engineering Research Institute (NEERI), Nagpur Area, Nagpur, India

RH	Relative humidity (%)
$\dot{S}$	Entropy (kJ kg^{-1} K^{-1})
T	Temperature (°C)
W	Work consumption (kW)
Y	Variables that represents COP, cooling capacity or exergy efficiency

Greek symbols

α	Percentage of refrigerant recover (%)
β	CO$_2$ emission factor
$\dot{\vartheta}$	Specific volume (m^3 kg^{-1})
ε	$\frac{Y_{\text{HFO}-1234\text{yf}} - Y_{\text{HFO}-134\text{a}}}{Y_{\text{HFO}-134\text{a}}}$
η	Efficiency (%)

Subscripts

comp	Compressor
cond	Condenser
d	Discharge
ele	Motor electrical power
evap	Evaporator
ex	Exergy
exp	Expansion device
gen	Generation
in	Inlet
L.S	Liquid side
O	Dead state
ot	Outlet
r	Refrigerant
ref	Reference state
V.S	Vapour side

Introduction

HFC-134a was evolved as a permanent replacement for CFC-12 and is being used for the past few decades. As global warming has become increasingly significant, it is important to limit and reduce the usage of high global warming potential (GWP) refrigerants [1]. As indicated by Kyoto protocol in 1997, HFC-134a was recognised as a controlled ozone depleting substance, and it has global warming potential of 1430. The Kigali Amendment to Montreal Protocol [2] was recommended to reduce the production and usage of the high GWP HFC refrigerants. In India, the usage of HFC-134a in new systems has been planned to be banned by 2028 with a servicing tail till 2047 (Article 5 parties, Group 2). In Europe, the MAC manufacturers have already banned the usage of HFC-134a in vehicles manufactured since 2016 due to the F-Gas regulations and fixed the maximum permissible limit of GWP in alternatives as 150 [3]. Therefore, it is necessary to select new alternative refrigerants having GWP less than 150 to substitute HFC-134a in mobile air conditioning (MAC) sector. The air conditioners in automobiles

consume 12–17% of its total power from the engine, and thus it has a significant role in the vehicle fuel consumption [4] and hence detailed energy efficiency enhancement studies are needed on the new refrigerants.

Refrigerants such as R-744, HFC-152a, hydrocarbons (HC-290 and HC-600a), and hydrofluoroolefins (HFO-1234ze and HFO-1234yf) have GWP less than 150, and they are the probable candidates to replace HFC-134a [5]. The natural refrigerant R-744 has a GWP of 1, but it has disadvantages of very high operating pressure and low critical temperature. Therefore, R-744 is not appropriate to be retrofit in existing HFC-134a system [6]. Tanaka and Higashi [7] have reported that HFO-1234yf is a possible candidate for retrofitting in HFC-134a system because of its similar thermo-physical properties and low GWP (<4). However, it has flammability issues and is classified under A2L as a mildly flammable substance in ASHRAE standard 34 [8]. Typical thermo-physical properties of HFC-134a and HFO-1234yf are shown in Table 1.

The trifluoroacetic acid (TFA) formation is a problem associated with the usage of HFO-1234yf in a MAC system when released/leaked into the atmosphere. The TFA is extremely resistant to reductive degradation and microbial oxidation. Therefore, this will accumulate in the water bodies over a long period of time, resulting in harmful effects on flora and fauna [9]. Lueken et al. [10] reported that the 100 µg L^{-1} of TFA concentration is found to be a safe level in the aquatic bodies and the direct inhalation of HFO-1234yf in atmosphere will not cause any health effects. Kajihara et al. [11] simulated the TFA formation due to the leakage of HFO-1234yf used in HFC-134a system, and it was revealed that the peak TFA levels were in the range between 1.26 and 1.70 µg L^{-1} only. Therefore, the effect of HFO-1234yf on the environment is very minimal and it is safe.

Lewandowski [12] reported that the HFO-1234yf has lower flammability index than that of the HFC-152a, HC

Table 1 Properties of refrigerant HFC-134a and HFO-1234yf at 5 °C

Properties	HFC-134a	HFO-1234yf
Saturated pressure/bar	349.66	372.92
Vapour density/kg m^{-3}	17.131	20.744
Liquid density/kg m^{-3}	1278.1	1160.4
Vapour enthalpy/kJ kg^{-1}	401.49	366.52
Liquid enthalpy/kJ kg^{-1}	206.75	206.5
Vapour Cp/kJ kg^{-1} K^{-1}	0.92059	0.94835
Liquid Cp/kJ kg^{-1} K^{-1}	1.3552	1.308
Vapour therm. cond./W m^{-1} K^{-1}	11.954×10^{-3}	12.044×10^{-3}
Liquid therm. cond./W m^{-1} K^{-1}	89.806×10^{-3}	73.422×10^{-3}
Vapour viscosity/Pa s	10.911×10^{-6}	11.363×10^{-6}
Liquid viscosity/Pa s	250.11×10^{-6}	197.1×10^{-6}
GWP	1430	4
Flammability	A1	A2L

refrigerants and their blends, and it was acceptable to be used in new MAC systems as well as in retrofitted systems. According to Environmental Protection Agency [13], the HFO-1234yf in the MAC systems must follow some safety requirements as per SAE J639 which includes compressor cut-in/cutoff switch, pressure relief devices, and other specific fittings.

Previous studies [14–16] revealed that the coefficient of performance (COP) and cooling capacity of vapour compression refrigeration (VCR) system with HFO-1234yf were 3–15% and 0.3–19%, respectively, lower than those with HFC-134a. Sukri et al. [17] stated that the liquid subcooling has the potential to improve the performance of a MAC system operated with HFO-1234yf and HFC-134a. Junye et al. [18] found that the MAC system performance with HFO-1234yf was poorer under retrofit condition. However, the tuning of thermostatic expansion valve (TXV) superheating resulted in better system performance. Zilio et al. [19] analysed the experimental performance of HFO-1234yf in a typical HFC-134a MAC system with a nominal cooling capacity of 5800 W. It was reported to have a poorer performance as a drop in substitute and suggested to have small hardware modifications such as TXV tuning and optimised variable displacement compressor to improve the system performance. Many researchers [20–24] suggested that the use of suction/liquid line heat exchanger (SLHX) and sub-cooler can improve the subcooling before the expansion process. The study made by Desai et al. [22] found that the HFC-134a system COP was improved by 7–12% with the introduction of SLHX. Navarro-Esbri et al. [23] and Cho et al. [24] reported that the difference in cooling capacity and COP between HFO-1234yf and HFC-134a can be reduced by up to 1.8% and 3%, respectively, by adopting SLHX.

Another great challenge for air conditioning engineers is to use minimum amount of power from the vehicle engine to reduce the fuel consumption and in turn NOx emissions. Kurata et al. [25] also observed that the SLHX implementation reduced the power consumption up to 10% for the same cooling capacity in HFC-134a MAC system, which indirectly reduces the fuel consumption. It is also very important to determine the optimal refrigerant charge to get maximum performance under any working condition. In MAC systems, the optimal charge is normally determined at some extreme operating conditions. Such conditions may vary with HVAC manufacturers, and it requires detailed thermodynamic analysis [26]. Many researchers carried out the charge optimisation test using energy analysis and it deals only with COP [27]. However, the exergy analysis is an useful method to analyse the actual system losses and their magnitude due to irreversibilities. This method gives a better understanding on the system performance and also indicates avenues to enhance the system efficiency [28].

Prabakaran and Lal [29] proposed an exergy-based charge optimisation method instead of COP-based method. It was found that the exergy method was more consistent and yielded single optimum charge irrespective of compressor speed. Golzari et al. [30] theoretically studied the MAC system performance with HFO-1234yf using second law of thermodynamics. They found that the exergy efficiency decreased with rise in evaporator/condenser air inlet temperature and drop in condenser air velocity. It was also found that the exergy efficiency and COP of HFO-1234yf were 19.8% and 15.5%, respectively, higher than that of existing HFC-134a. They also found that the majority of the losses occurred in the compressor, trailed by the condenser, expansion device and lastly the evaporator. Recently, the environmental impacts because of the air conditioning and refrigeration system operation have been taken account seriously due to the global warming effect [31]. There are numerous techniques used to assess the environmental impact associated with air conditioning and refrigeration systems namely GWP, total equivalent warming impact (TEWI), carbon footprints and life cycle climate performance (LCCP) [32]. Abraham and Mohanraj [33] reported the TEWI analyses of the MAC systems using R430A and HFC-134a. They found that the system with R430A had 35%, 32.4% and 47.3% lower TEWI than those of the system using HFC-134a for petrol, diesel and liquid petroleum gas vehicles, respectively,

Mastrullo et al. [34] reported the performance of MAC unit in a high-speed train based on TEWI and energy consumption using HFO-1234yf, HFO-1234ze, and HFC-134a. The results showed that the TEWI of HFO-1234yf and HFO-1234ze were 5% and 18% lower than HFC-134a system during summer condition. Aprea et al. [35] analysed the global effects of R-744 as a replacement for HFC-134a in the refrigeration system using TEWI analysis. The results showed that the indirect emission from the trans-critical R-744 system was always higher than the baseline HFC-134a system due to its low cycle efficiency. The TEWI index was 5–22% lower for HFC-134a in comparison with R-744 (at a fixed leakage rate between 5 and 20%) for MAC system.

It can be realised that many researchers reported that the performance of MAC systems with HFO-1234yf can be enhanced by the inclusion of SLHX [21–24] and tuning the TXV [18–20]. However, no study has been reported by combining the SLHX and suitable TXV tuning in the same system to improve the HFO-1234yf system performance. The novelty of the present study is to analyse the effect of TXV tuning on the MAC system performance enhancement with SLHX using HFO-1234yf as a replacement for HFC-134a at different compressor speeds. Initially, charge optimisation test was carried out for HFC-134a and HFO-1234yf at idling speed (900 rpm). The performance of the system as a function of refrigerant charge and compressor speeds are also evaluated based on energy as well as exergy

analysis. Further, the TXV superheat setting was tuned to enhance the performance of the MAC system in steps of 45° in the counter-clockwise direction. Finally, the environmental issues associated with MAC system was also evaluated by using TEWI analysis.

Experimental

Test facilities

The MAC system performance was carried out using a bench test rig schematically shown in Fig. 1, and the photographic view of complete test facilities is shown in Fig. 2. It consists of a 160 cc swash plate compressor, integrated receiver dryer (IRD) condenser ($590 \times 444.8 \times 16$ mm), mini channel evaporator ($230 \times 201 \times 38$ mm), block-type TXV and double-pipe SLHX ($L = 450$ mm). The evaporator coil with HVAC panel was fixed in the calorimetric chamber, and the compressor was operated by using a 3 phase 2 HP motor through a belt drive. The variable frequency drive (VFD) was used to vary the speed of the motor from 100 to 3000 rpm. Generally, the compressor operation is regulated by the thermostat switch and it works based on the supply air temperature. In order to conduct experiments under steady state, the thermostat was not used.

The requited airflow across the cooling coil was varied by varying the blower speed with a help of regulated power supply (RPS) and the condenser air flow rate was also regulated by a separate VFD that drives the condenser blower. The required chamber temperature and relative humidity (35 °C and 40% RH) were achieved by modulating the electrical heater power supply (via dimmer stat) and ultrasonic humidifier, respectively. All the refrigerant pipelines connecting the components were perfectly insulated. The required condenser inlet air temperature was also realised by providing heaters in the air inlet duct.

Measurements

The refrigerant temperature and pressure across each component were measured by using PT-100 type RTDs (± 0.15 °C) and MEAS pressure transmitters (± 2%), respectively. The refrigerant flow rate was measured with a help of Coriolis type (Promass 83, ± 0.15%, Make: Endress & Hausser) flow meter, which was fixed at the condenser outlet. The velocity of the airflow through the condenser and evaporator was measured using vane-type anemometer (± 5%). The compressor motor power consumption and speed were measured using an ELTRAC power meter (± 0.5%) and non-contact type tachometer (± 0.05%). All the measuring facilities except tachometer and power meter were connected into the data logger.
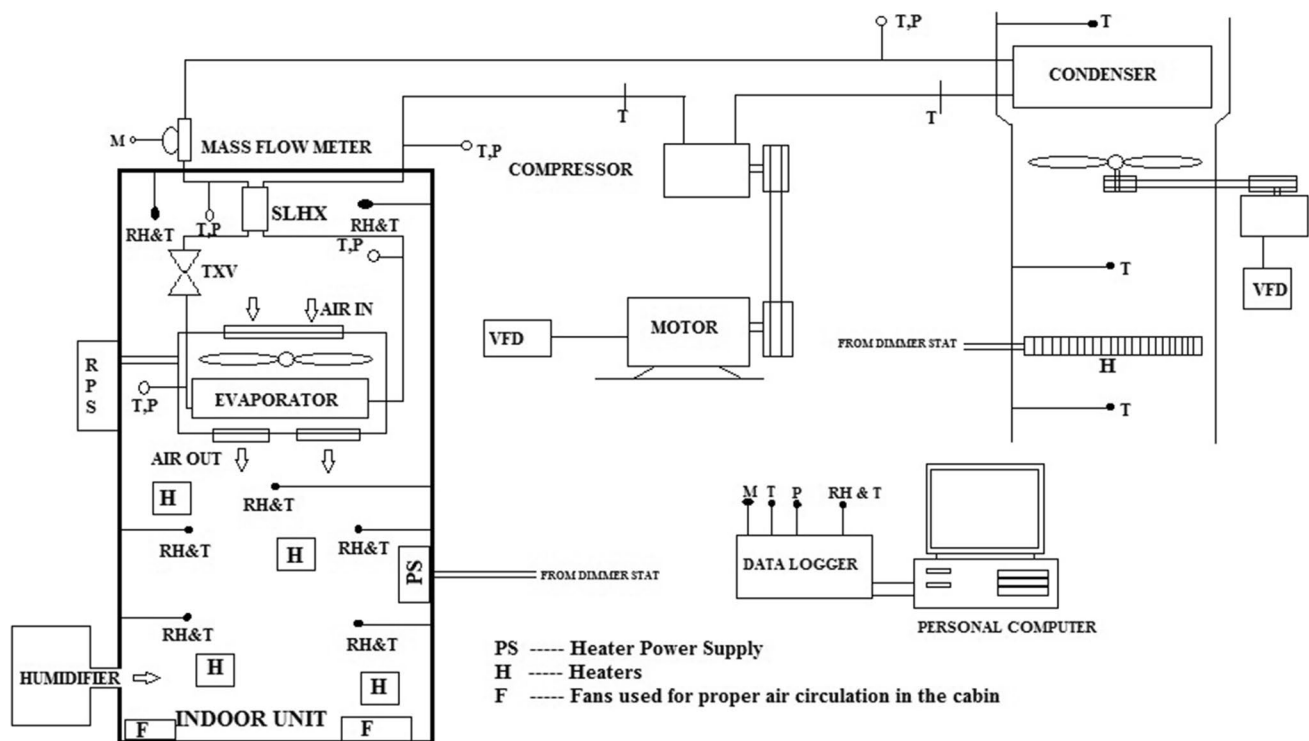

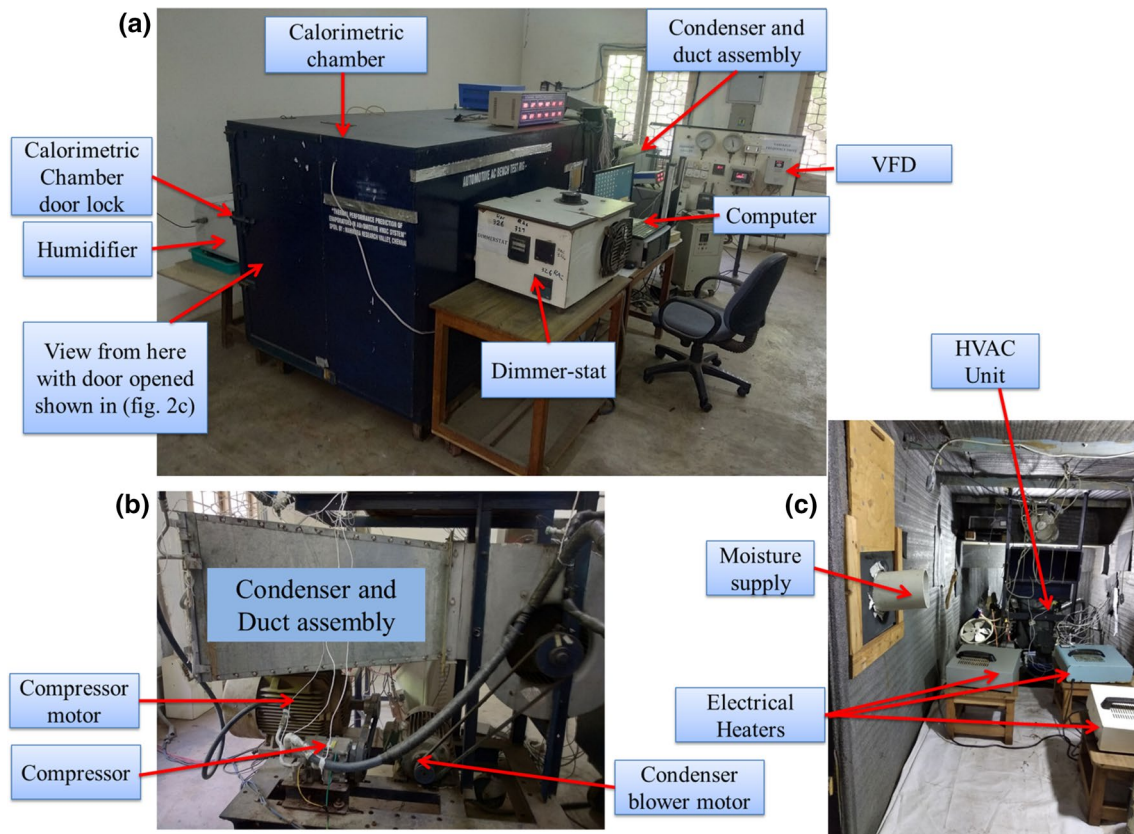**Fig. 1** Schematic of MAC system experimental facility

Fig. 2 Photographic view of test facility **a** overview of the facilities, **b** compressor and condensing unit assembly, **c** inside view of calorimetric chamber (door opened)

Table 2 Test condition for charge optimisation of MAC system

Compressor speed/rpm	Evaporator side		Condenser side	
	Air inlet condition	Air flow rate	Air inlet condition	Air face velocity
900	35/ °C and RH 40/%	420/m³ h⁻¹	35/ °C	2.5/m s⁻¹

Test conditions

The optimum charge identification is very important for all the refrigeration and air conditioning system for achieving maximum performance. The charge optimisation test was performed in the bench test rig itself. Compared to the real MAC systems, the length of the connecting hoses in the test rig is longer because of the measuring instruments. Though, it does not influence the system performance comparison because both the refrigerants are charged in the same system under retrofit condition. In this work, the test conditions for charge optimisation as shown in Table 2 were chosen as recommended by the Society of Automotive Engineers SAE J2765 standard [36]. Qi et al. [26] and Prabakaran and

Lal [29] were also used the same test conditions for charge optimisation.

The influences of compressor speed on the system performance are carried out for three different speeds of the compressor; viz, (1) Idling (900 rpm), (2) city limit (1800 rpm) and (3) high-speed conditions (2700 rpm). These conditions were chosen based on the study reported by Qi et al. [26].

Experimental

At first, the condenser and evaporator blower motors were switched ON through respective VFDs and then the required flow rates were achieved by regulating the VFD and RPS, respectively. Then HFC-134a refrigerant (initially 500 grams) was charged into the MAC system. The compressor motor, electrical heaters and humidifier were switched ON. After a few minutes, the magnetic clutch of the compressor was energised and connected to the motor shaft via a belt drive. The electrical heating loads were modulated using a dimmer stat to attain the required condition shown in Table 2. Small fans fixed in the calorimetric chamber were also switched ON for keeping constant temperature and RH throughout the chamber. After achieving the steady state,

the unit was permitted to run for 30 min. Then the following performance parameters namely (1) refrigerant temperature and pressure across each components, (2) mass flow rate of refrigerant, (3) RH and temperature of the air across the evaporator, (4) air temperature across the condenser, (5) temperature and RH in the calorimetric chamber and (6) compressor motor electrical power consumption were logged into the computer for another 30 min at 10 s interval. Further, the refrigerant was charged in steps of 30 g and then the same technique was repeated to find the optimum charge level.

With the same optimum charge, the experiment was repeated for three different compressor speeds of 900, 1800 and 2700 rpm for analysing the system performance The entire procedure was repeated with HFO-1234yf refrigerant with charges from 430 to 730 g insteps of 30 g.

Data reduction

The performance parameter of the MAC system based on the energy analysis is the COP. The MAC system actual COP is calculated based on the system cooling capacity (Q_{evap}) and the consumed power by the compressor motor (W_{ele}). The cooling capacity is the product of mass flow rate of the refrigerant $(\dot{m}_r)$ and the refrigerant enthalpic difference across the cooling coil [37],

$$COP = \frac{Q_{evap}}{W_{ele}} \tag{1}$$

The following equation was used to evaluate the volumetric efficiency of the compressor,

$$Volumetric\ efficiency = \frac{\dot{m}_r \vartheta_{r,in}}{CC \times compressor\ speed} \tag{2}$$

The maximum work that can be produced by a system or a process at a specified condition is called as exergy. In a process or a system, the losses occur due to the entropy generation [38]. The exergy balance during a process can be stated in the following equation [39],

$$ED = \left(\dot{E}_{in} - \dot{E}_{ot}\right) \tag{3}$$

where ED is the rate of exergy destruction and $\dot{E}_{in} - \dot{E}_{ot}$ is total exergy transferred during the process. It is can be explained in terms of entropy generation also

$$ED = T_o \dot{S}_{gen} \tag{4}$$

where T_o is the reference temperature for the considered process and $\dot{S}_{gen}$ is the entropy generated during the process.

The exergy destruction for the individual components of the MAC is as follows:Compressor,

$$ED_{comp} = \dot{W}_{ele} - \dot{m}_r\left(\left(h_{comp,ot} - h_{comp,in}\right) - T_o\left(s_{comp,ot} - s_{comp,in}\right)\right) \tag{5}$$

Condenser,

$$ED_{cond} = \dot{m}_r T_o\left(s_{cond,ot} - s_{cond,in}\right) + Q_{cond}\left(\frac{T_o}{T_{cond,ot}}\right) \tag{6}$$

SLHX,

$$ED_{SLHX} = \left(ED_{SLHX}\right)_{L,S} + \left(ED_{SLHX}\right)_{V,S} \tag{7}$$

$$\left(ED_{SLHX}\right)_{L,S} = \left(\dot{m}_r T_0\left(s_{slhx,ot} - s_{slhx,in}\right) - \frac{Q_{SLHX}}{T_{r,cond}}\right)_{L,S} \tag{8}$$

$$\left(ED_{SLHX}\right)_{V,S} = \left(\dot{m}_r T_0\left(s_{slhx,ot} - s_{slhx,in}\right) - \frac{Q_{SLHX}}{T_{r,evap}}\right)_{V,S} \tag{9}$$

Expansion device,

$$ED_{exp} = \dot{m}_r T_o\left(s_{exp,ot} - s_{exp,in}\right) \tag{10}$$

Evaporator,

$$ED_{evap} = \dot{m}_r T_o\left(s_{evap,ot} - s_{evap,in}\right) - Q_{evap}\left(\frac{T_o}{T_{evap,ot}}\right) \tag{11}$$

The exergy efficiency of the VCR system is defined as follows:

$$\eta_{ex} = \frac{COP_{actual}}{COP_{carnot}} \tag{12}$$

The thermo-physical properties of the refrigerants HFO-1234yf and HFC-134a were taken from the REFPROP software [40].

Uncertainty analysis

The measured parameters such as refrigerant side temperature/pressure across each component, mass flow rate of refrigerant, compressor speed, compressor power consumption are used to estimate the system cooling capacity, COP, and exergy efficiency. The uncertainties of estimated parameters are calculated by using the following equations, which are derived from Moffat method [41] and the values are tabulated in Table 3.

$$Q_{evap} = f\left(\dot{m}_{ref}, T_{evap.in}, T_{evap.ot}, P_{evap,in}, P_{evap,ot}\right) \tag{13}$$

Table 3 Uncertainties of estimated parameters

Estimated parameters	Uncertainties/%	
	HFC-134a	HFO-1234yf
Cooling capacity	±2.14	±2.17
Compressor power	±1.62	±1.63
COP	±2.09	±2.35
Exergy efficiency	±2.54	±2.68

with increase in refrigerant charge, while DSC increases for both the systems owing to the increased refrigerant flow rate and higher condensing temperature. At a lower charge, TXV cannot control the flow rate because it is already in fully opened position due to higher DSH, while the associated higher discharge pressure results in increased mass flow rate through the TXV leading to drop in DSH. This is experienced for a refrigerant charge up to 600 g and 650 g for HFO-1234yf and HFC-134a, respectively.
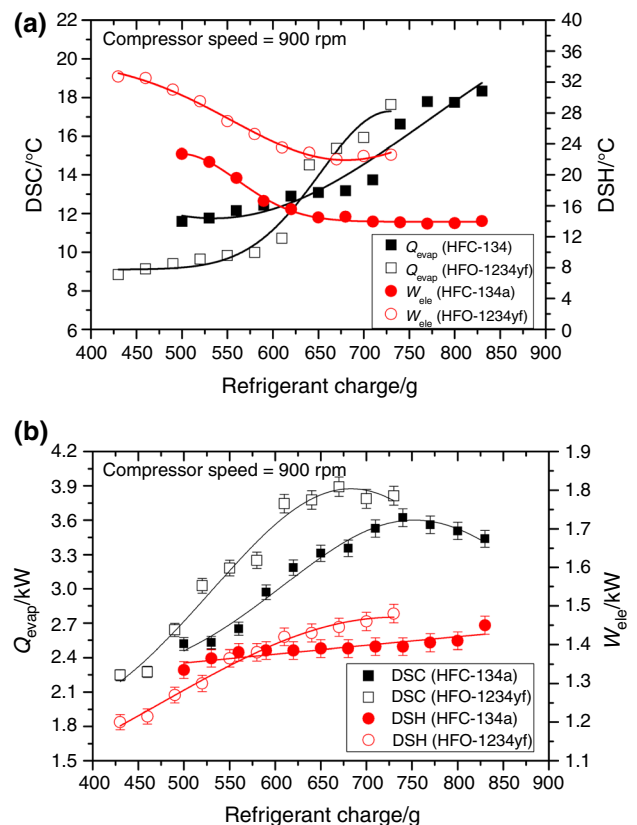
$$\frac{\partial Q_{\text{evap}}}{Q_{\text{evap}}} = \sqrt{\left(\frac{\partial T_{\text{evap,in}}}{T_{\text{evap,in}}}\right)^2 + \left(\frac{\partial T_{\text{evap,ot}}}{T_{\text{evap,ot}}}\right)^2 + \left(\frac{\partial P_{\text{evap,in}}}{P_{\text{evap,in}}}\right)^2 + \left(\frac{\partial P_{\text{evap,ot}}}{P_{\text{evap,ot}}}\right)^2 + \left(\frac{\partial \dot{m}_{\text{ref}}}{\dot{m}_{\text{ref}}}\right)^2} \tag{14}$$

$$W_{\text{comp}} = f\left(\dot{m}_{\text{ref}}, T_{\text{comp.in}}, T_{\text{comp.ot}}, P_{\text{comp,in}}, P_{\text{comp,ot}}, W_{\text{ele}}\right) \tag{15}$$

$$\frac{\partial W_{\text{comp}}}{W_{\text{comp}}} = \sqrt{\left(\frac{\partial T_{\text{comp,in}}}{T_{\text{comp,in}}}\right)^2 + \left(\frac{\partial T_{\text{comp,ot}}}{T_{\text{comp,ot}}}\right)^2 + \left(\frac{\partial P_{\text{comp,in}}}{P_{\text{comp,in}}}\right)^2 + \left(\frac{\partial P_{\text{comp,ot}}}{P_{\text{c,o}}}\right)^2 + \left(\frac{\partial \dot{m}_{\text{ref}}}{\dot{m}_{\text{ref}}}\right)^2 + \left(\frac{\partial W_{\text{ele}}}{W_{\text{ele}}}\right)^2} \tag{16}$$

$$\text{COP}_{\text{actual}} = f\left(Q_{\text{evap}}, W_{\text{comp}}\right) \tag{17}$$

$$\frac{\partial \text{COP}_{\text{actual}}}{\text{COP}_{\text{actual}}} = \sqrt{\left(\frac{\partial Q_{\text{evap}}}{Q_{\text{evap}}}\right)^2 + \left(\frac{\partial W_{\text{comp}}}{W_{\text{comp}}}\right)^2} \tag{18}$$

$$\eta_{\text{ex}} = f\left(\text{COP}_{\text{actual}}, \text{COP}_{\text{carnot}}\right) \tag{19}$$

$$\frac{\partial \eta_{\text{ex}}}{\eta_{\text{ex}}} = \sqrt{\left(\frac{\partial \text{COP}_{\text{actual}}}{\text{COP}_{\text{actual}}}\right)^2 + \left(\frac{\partial \text{COP}_{\text{carnot}}}{\text{COP}_{\text{carnot}}}\right)^2} \tag{20}$$

Results and discussion

Based on the measured variable, the MAC system performance parameters such as degree of superheating (DSH), degree of subcooling (DSC), compressor power consumption, cooling capacity and system COP were calculated at each charge level for HFO-1234yf and HFC-134a systems. Further, the components exergy destructions and exergy efficiency at each level of the refrigerant charge were also estimated. Finally, the effect of TXV tuning on the HFO-1234yf system performance improvement was also presented.

Energy analysis

The variations in DSH and DSC for the different refrigerant charges are shown in Fig. 3a. It shows that the DSH reduces

Fig. 3 Influences of refrigerant charge on **a** DSC at TXV inlet and DSH at compressor inlet, **b** cooling capacity and compressor power consumption

At this point, DSH reaches the safe level and the system starts running smoothly. This charge is said to be "minimum effective charge" for the individual system [26]. Further charge addition will lead to a plateauing effect in DSH as well as DSC in HFC-134a while the DSH slightly increases for HFO-1234yf. This could be due to the variation in saturation pressure between the operating fluid (HFO-1234yf) and the bulb fluid (HFC-134a) in the TXV which results in reduced HFO-1234yf mass flow rate, whereas the same is by and large steady for HFC-134a. The DSH in the HFC-134a system is almost the same between the charges of 710–800 g, and DSC is the same between the charges of 710–740 g. Then further charging increases DSC suddenly by 1 °C. The same trend is also experienced in HFO-1234yf system between the refrigerant charges of 640–670 g. The low latent heat of vaporisation of HFO-1234yf causes quick evaporation of the refrigerant resulting in higher DSH and correspondingly more refrigerant flow rate ranging from 23.6 to 44.7% in comparison with HFC-134a.

The variation in the cooling capacity and power consumption of the compressor motor as a function of refrigerant charge are presented in Fig. 3b. The cooling capacity increases with a refrigerant charge up to 740 g and 670 g in HFC-134a and HFO-1234yf system, respectively. Beyond this charge, it starts decreasing because of the reduced refrigerant mass flow rate, while the compressor motor power consumption increases continuously with refrigerant charge. The maximum cooling capacity and the corresponding compressor motor power consumption of HFO-1234yf system are 7.43% and 3.58% higher when compared to HFC-134a system. At this point, the HFO-1234yf has 26% higher mass flow rate when compared to HFC-134a, whereas the discharge pressure dropped by 2.57%. The reason behind the higher HFO-1234yf mass flow rate is its higher vapour

density when compared to HFC-134a. The lower discharge pressure in HFO-1234yf system is resulting from its lower vapour pressure for the same saturation temperature than that of HFC-134a system. When compared to HFC-134a, the latent heat of evaporation of HFO-1234yf is low; though it has higher cooling capacity owing to its higher mass flow rate.

The variation in COP of the HFC-134a and HFO-1234yf systems as function of refrigerant charge is shown in Fig. 4. The trend of COP variation is like that of the cooling capacity for both the systems. The maximum COP is experienced at 670 g and 740 g for the HFO-1234yf and HFC-134a systems, respectively. This is observed to be the "Optimum charge" of the individual refrigerants. The reduced value of the optimum charge of HFO-1234yf is owing to its lower liquid density. At this point, the COP of HFO-1234yf system is 3.71% higher than that of HFC-134a system. The rise in cooling capacity outweighs the rise in compressor power resulting in higher COP for HFO-1234yf system.

Exergy analysis

The exergy efficiency of the MAC system depends on the exergy destructions experienced in the each component used in the system. According to the Cho and Park [27] and Prabakaran and Lal [29], the compressor has more exergy destruction and it decides the performance of the system. Therefore, the compressor exergy destruction along with system exergy efficiency for various refrigerant charges is presented in Fig. 5.

As refrigerant charge increases from 500 to 560 g in HFC-134a system and 430–580 g in HFO-1234yf system, the compressor exergy destruction increases because of the higher DSH at compressor inlet. Further increase in charge reduces the loss in the compressor up to 740 g and 640 g
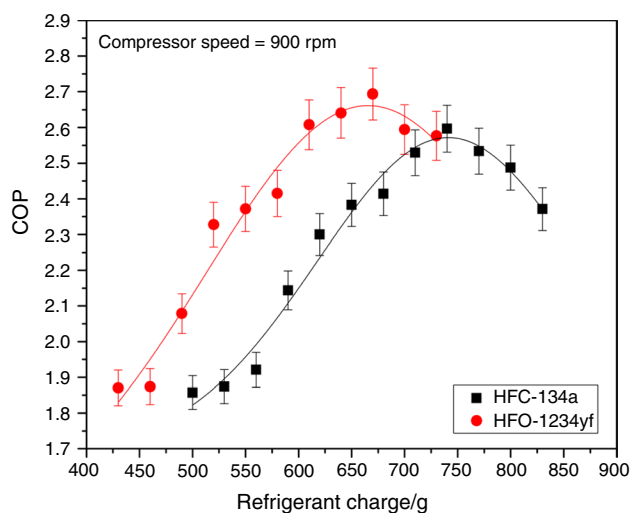

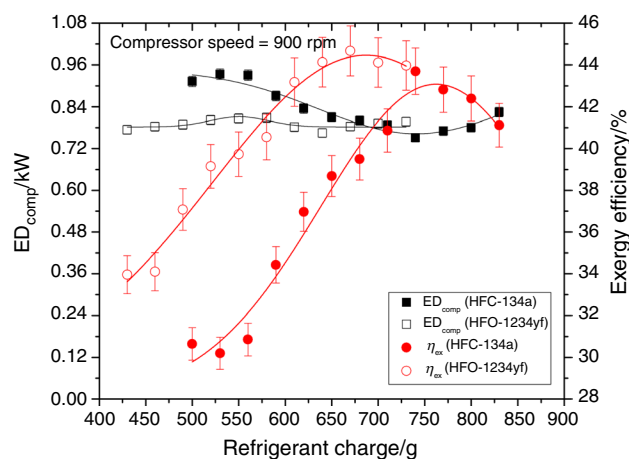**Fig. 4** Influence of refrigerant charge on the system COP

Fig. 5 Influences of refrigerant charge on the exergy destruction in compressor and exergy efficiency of the system

in HFC-134a and HFO-1234yf system, respectively, due to the drop in DSH and improved refrigerant flow rate. Comparing these points, the exergy destruction experienced in the HFO-1234yf system compressor is 4.28% higher than that of HFC-134a system compressor. Beyond this charge, the losses in the compressor increases in both the system because of the excess charge that has accumulated in the condenser resulting in higher discharge pressure and lower refrigerant mass flow rate.

The trend of the exergy efficiency variation as a function of charge quantity of the refrigerant for both the refrigerants is similar to that of the system cooling capacity and the system COP as shown in Figs. 3b, and 4, respectively. The exergy efficiency increases with a refrigerant charge up to 670 g and 740 g for HFO-1234yf and HFC-134a systems, respectively, and beyond that, it starts decreasing. The maximum exergy efficiency of 39.1% and 40.1% is experienced in HFC-134a and HFO-1234yf system. The maximum exergy efficiency of HFO-1234yf system is 2.57% higher than that of HFC-134a system, which is also reflected in the trend of actual COP.

From the analysis, it is found that the trends of exergy destruction experienced in the evaporator, TXV, condenser and compressor with respect to refrigerant charge are similar to the results reported by Prabakaran and Lal [29] using HFC-134a in MAC system without SLHX.

At the optimum charge, the condenser exergy destruction in the HFO-1234yf system is 14.97% lower than that of HFC-134a system due to its lower discharge pressure, while in the TXV, evaporator, and SLHX, it is higher by 115.17%, 28.51%, and 25.7%, respectively. It is to be noticed that the saturation pressure of HFO-1234yf is higher at a lower temperature which becomes lower than HFC-134a above 40 °C. The increased refrigerant mass rate and higher DSH result in more destruction in the TXV and the evaporator,

respectively. The excess mass flow rate is due to the difference in the saturation pressure between bulb fluid (HFC-134a) and the working fluid (HFO-1234yf) when the HFC-134a system is retrofitted with HFO-1234yf.

Influences of compressor speed on the performance of the system

The system COP and exergy efficiency were analysed with the optimum charge in both the systems by varying the compressor speed. Three speeds namely 900, 1800 and 2700 rpms were considered. The change in compressor discharge temperature and discharge pressure for the various compressor speeds are shown in Fig. 6. It is found that the discharge temperature and the pressure increase when compressor speed increased from 900 to 2700 rpm. As the speed is increased from 900 to 2700 rpm, the rise in discharge pressure of HFC-134a and HFO-1234yf is found to be 22.75% and 25.37%, while the discharge temperature is increased by 31.72% and 29.11%, respectively. When compressor speed increased from 900 to 2700 rpm, the difference in discharge temperatures of HFC-134a and HFO-1234yf system increases, whereas the difference in discharge pressure decreases. This can be attributed to the pressure–temperature characteristics of the two fluids. It also shows that

Table 4 Compression ratio and volumetric efficiency of the compressor as a function of compressor speed

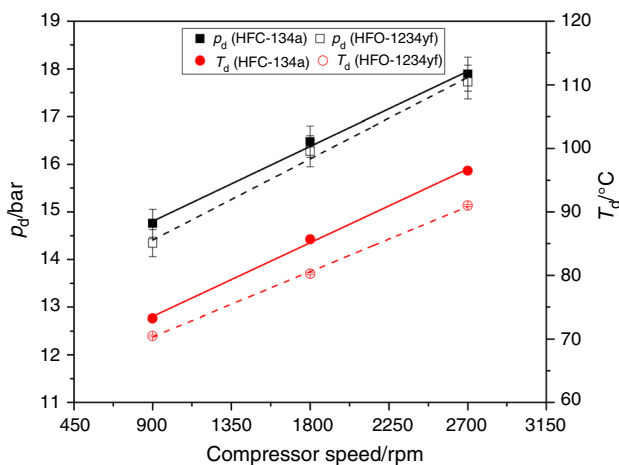| Compressor speed/rpm	Compression ratio		Volumetric efficiency	
	HFC-134a	HFO-1234yf	HFC-134a	HFO-1234yf
900	3.73	3.38	0.522	0.562
1800	5.25	4.71	0.453	0.486
2700	5.76	5.24	0.362	0.388

Fig. 6 Influences of compressor speed on discharge pressure and discharge temperature
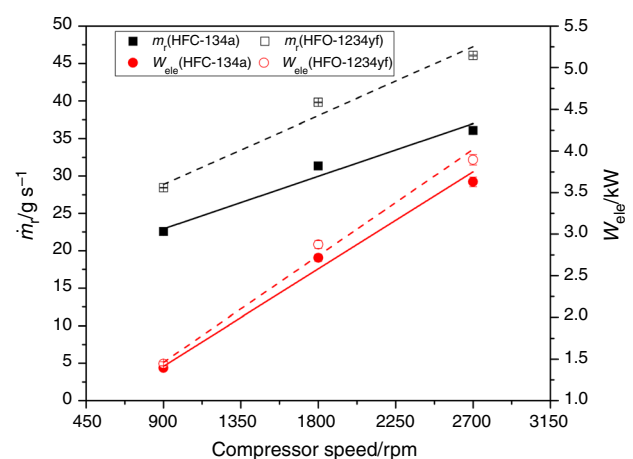

Fig. 7 Influence of compressor speed on refrigerant mass flow rate and compressor power consumption

the HFO-1234yf system has 0.98–3.03% of lower discharge pressure than HFC-134a as the speed is varied from 900 to 2700 rpm. The reason behind the lower discharge pressure of HFO-1234yf is its lower vapour pressure.

The variation in the pressure ratio and the compressor volumetric efficiency as a function of compressor rpm are shown in Table 4. It is observed that the pressure ratio increases with compressor speed and hence the volumetric efficiency reduces for both the refrigerants. It also shows that the HFO-1234yf system pressure ratio is 9.02–10.30% lower than that of HFC-134a system, while the volumetric efficiency was higher by up to 7.66%. The reduced discharge pressure by up to 3.03% resulted in lower pressure ratio for HFO-1234yf.

The variations in refrigerant mass flow rate and compressor power consumption as a function of compressor speed for HFC-134a and HFO-1234yf are shown in Fig. 7. The refrigerant flow rate and the compressor power consumption increases with increase in compressor speed for both the systems. As the speed increased from 900 to 2700 rpm, the increase in mass flow rate of HFC-134a and HFO-1234yf is found to be 59.88% and 62.02%, respectively, while the compressor power increases by 160.21% and 169.55%. Overall, the mass flow rate and compressor power consumption are higher for HFO-1234yf at all the speeds by 26–27.6% and 4–7.3%, respectively, than those of HFC-134a. The specific volume and latent heat of vaporisation of the HFO-1234yf are lower than those of HFC-134a at the same saturation pressure resulting in more refrigerant mass flow rate at the same compressor speed for HFO-1234yf. A lower pressure ratio for HFO-1234yf results in a better volumetric efficiency which increases the pumping capacity. This effect coupled with lower vapour specific volume yields a higher mass flow rate. Further the lower latent heat of vapourisation results in higher DSH leading to more opening of the TXV. This also

complements the mass flow rate along with the compressor pumping power. The reason behind the higher power consumption in case of HFO-1234yf is owing to its high DSH at compressor inlet and higher refrigerant mass flow rate compared to HFC-134a. Rajendran et al. [38] also reported that the refrigerant mass flow rate and power consumption of HFO-1234yf system was 16–24% and 3–14% higher than those of HFC-134a system for a given compressor speed.

The influence of the compressor speed on the system COP and cooling capacity are shown in Fig. 8. It is found that the system cooling capacity increases with compressor speed, whereas the COP reduces for both the systems. The increase in the cooling capacity of HFC-134a and HFO-1234yf systems is found to be 63.21% and 48.37%, respectively, while the COP reduced by 37.31% and 44.94%. The HFO-1234yf system has 7.43% and 4.01% higher cooling capacity than that of HFC-134a system at a compressor speed range of 900 and 1800 rpm, respectively. Although the latent heat of evaporation of HFO-1234yf is low when compared HFC-134a, it has higher cooling capacity resulting from better heat transfer between the refrigerant inside the cooling coil and the cabin air due to the improved refrigerant mass flow rate. At high compressor speed of 2700 rpm, HFO-1234yf system cooling capacity is lower than that of HFC-134a system by 2.33%. This could be due to the rise in mass flow rate which is not sufficient enough to compensate for the lower latent heat of HFO-1234yf. Similar trends are experienced in COP variations also. At a lower speed of 900 rpm, the HFO-1234yf system COP is 3.71% higher than that of HFC-134a system, whereas it reduced by 1.743% and 8.97% for compressor speed of 1800 and 2700 rpm, respectively. The reason behind the lower COP is that the increase in cooling capacity doesn't equivalent with the magnitude of the rise in compressor motor power consumption as compressor speed is increased.
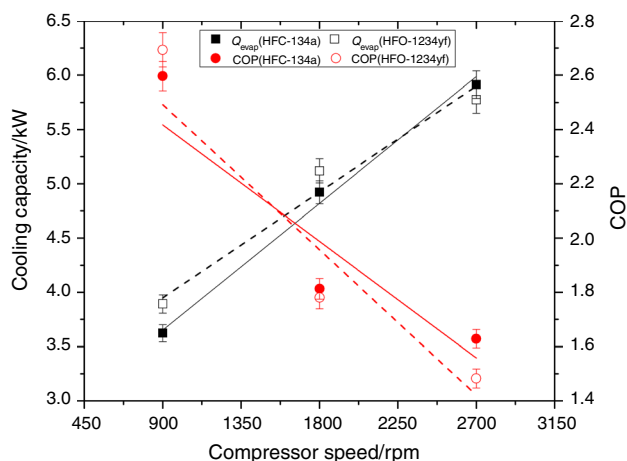

Fig. 8 Influences of compressor speed on cooling capacity and COP of the system
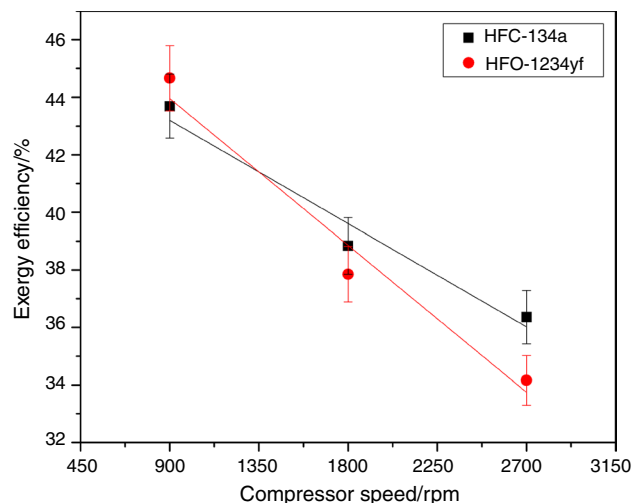

Fig. 9 Influence of compressor speed on exergy efficiency of the system

The influence of the compressor speed on the system exergy efficiency is shown in Fig. 9. It shows exergy efficiency of the HFC-134a and HFO-1234yf systems is reduced by 14.18% and 20.81%, respectively, as compressor rpm increases from 900 to 2700 rpm. At low speed of 900 rpm, the HFO-1234yf system exergy efficiency is 2.57% higher, whereas the HFC-134a system performs better at higher rpms namely 1800 and 2700. The exergy efficiency of HFC-134a is higher by 5.35% at 2700 rpm. The higher COP of HFC-134a leads to increase in the exergy efficiency at higher speeds. From this study, it is evident that the HFO-1234yf MAC system with SLHX gives better performance than that of HFC-134a at low compressor speed using optimum refrigerant charge and slightly poor performance at higher compressor speed.

The influence of the compressor speed on the DSH and DSC for different compressor speeds is tabulated in Table 5. As the speed increases the DSH reduces for both the refrigerants, but it is well above the normal DSH value if HFO-1234yf is used, while the DSC increased. Despite the fact that the mass flow rate of HFO-1234yf is high, the DSH is almost 12 °C higher than that of HFC-134a; this is because of the lower latent heat of evaporation and improper expansion process. Zilio et al. [19] and Zhao [42] have also reported similar kind of experimental results when HFO-1234yf was used in the existing HFC-134a MAC system without SLHX.

It may be noted that the DSH at suction would be still higher because of the exchange of heat in the SLHX (as seen from Fig. 3a) and hence the performance of HFO-1234yf comes down at higher speeds. This gives a clue that the superheat setting is to be tuned so that the mass flow rate increases and the suction superheat get reset to the original value. This can improve the performance of the evaporator as well as the compressor. Needless to say that the exergy destruction would be decreased and the exergy efficiency also would increase.

Effect of TXV tuning on system performance with HFO-1234yf

The TXV orifice opening is controlled by evaporator outlet pressure, the spring force (adjustable superheat setting)

Table 5 DSH and DSC as a function of compressor speed

Compressor speed/rpm	DSH at Evaporator outlet/°C		DSC at TXV inlet/°C	
	HFC-134a	HFO-1234yf	HFC-134a	HFO-1234yf
900	3.5	18.1	16.6	15.4
1800	2.4	15.4	18.9	16.2
2700	1.5	14.5	20.2	17.4

and sensing bulb pressure. Normally, all the manufactured TXVs are provided with a superheat values between 6 and 12 °C of DSH; that is sufficient for most applications. However, as seen in the previous sections, the inclusion of SLHX increases the DSH at the compressor inlet and the system with HFO-1234yf has higher DSH than that of HFC-134a by 12 °C. Junye et al. [18] and Rajendran et al. [20] have suggested tuning the TXV for reducing the DSH in order to improve performance. Therefore, the TXV was tuned by opening the orifice to increase the mass flow rate that reduces the DSH at the evaporator outlet. This was done by turning the TXV superheat adjusting screw counter-clockwise in steps of 45°, and angle of turn is further referred as tuning angle. The outcome of TXV tuning on the HFO-1234yf system performance is discussed below. The maximum opening was limited to 180° of turning the screw as there was sufficient mass flow rate that significantly reduced the DSH at the cooling coil exit.

The effect of TXV tuning angle on the refrigerant mass flow rate, DSH at evaporator outlet and compressor inlet of the HFO-1234yf system is shown in Fig. 10. It shows that the HFO-1234yf mass flow rate increases as the TXV orifice open for all the compressor speeds, resulting in the drop of the DSH at both compressor inlet and evaporator outlet. When superheat adjusting screw rotates in counter-clockwise, the spring pressure acting on the diaphragm reduces and this allows the valve stem goes downwards resulting in more opening in the TXV orifice. With 180° TXV tuning, the maximum increase in the HFO-1234yf mass flow rate is found to be 10.6%, 13.9% and 10% at a compressor speeds of 900, 1800 and 2700 rpm, respectively, while DSH at evaporator outlet reduced by 6 °C, 6.1 °C and 6.5 °C. Similarly, the DSH at compressor inlet drops by 3.2 °C, 4 °C and 5.6 °C at a compressor speed of 900, 1800 and 2700 rpms, respectively. The increase in mass flow is reduced at 2700 rpm, as compared to other two speeds, which indicates that the full flow of refrigerant through the TXV may be reached and the tuning was stopped after 180° in counter-clockwise. Rajendran et al. [20] also reported that the TXV tuning by 180° resulting in improved refrigerant mass flow rate leads to a drop in DSH at compressor inlet by 7 °C in HFC-134a MAC system.

The variation in compressor power consumption, cooling capacity COP, and exergy efficiency of HFO-1234yf system for the various TXV tuning angle is shown in Fig. 11. It shows that TXV tuning has positive effects on both COP and cooling capacity; however, the power consumption increases continuously due to the higher HFO-1234yf mass flow rate. The increase in refrigerant mass flow rate reduced the DSH at the evaporator outlet which in turn reduces the two phase heat transfer length in the evaporator resulting in better heat transfer between the refrigerant and the cooling air. With 180° tuning, the maximum enhancement in

Fig. 10 Effect of TXV tuning on **a** refrigerant mass flow rate and **b** DSH at evaporator outlet and compressor inlet
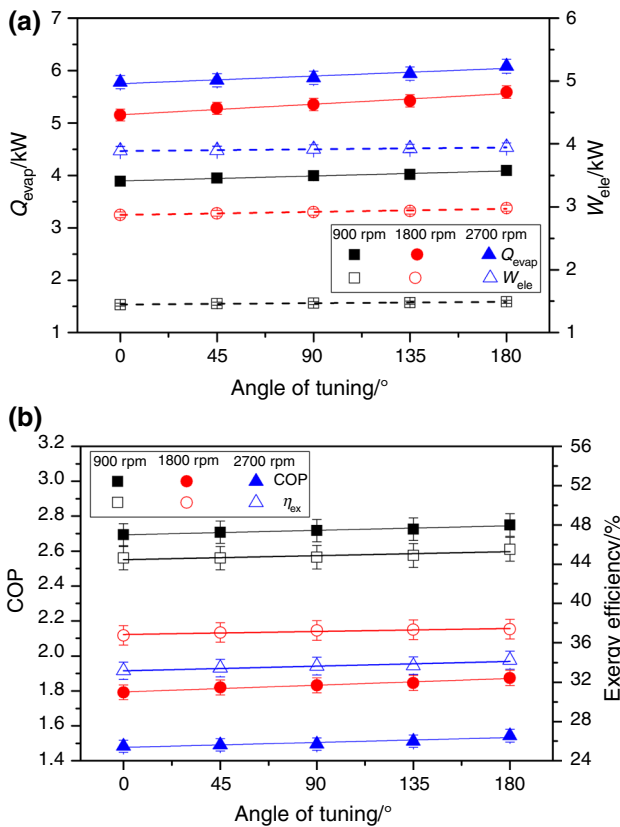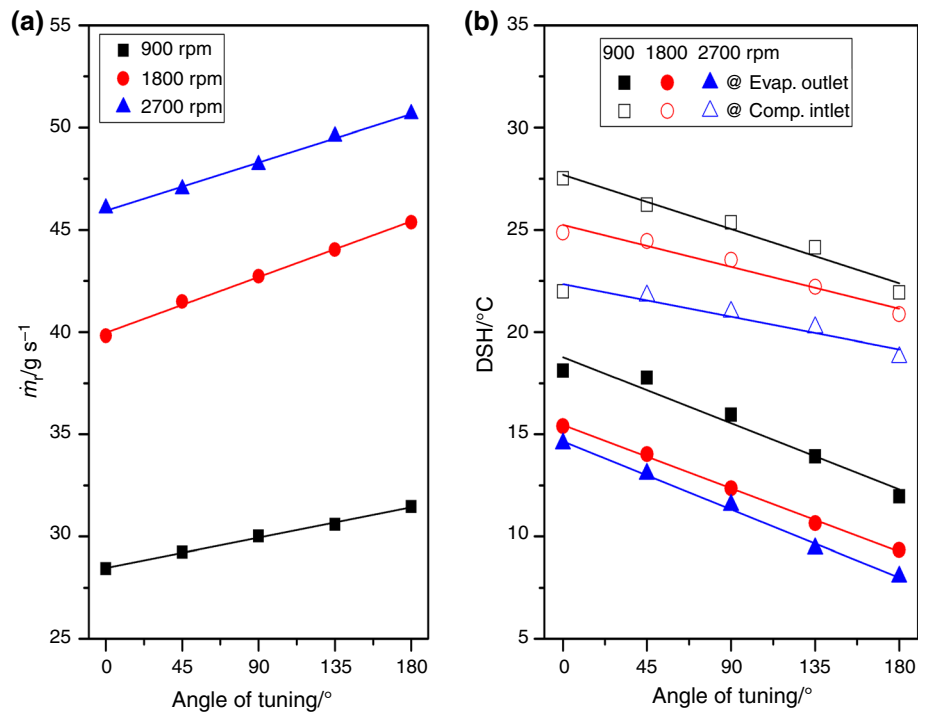

Fig. 11 Effect of TXV tuning on **a** Cooling capacity and compressor power consumption, **b** COP and Exergy efficiency of HFO-1234yf
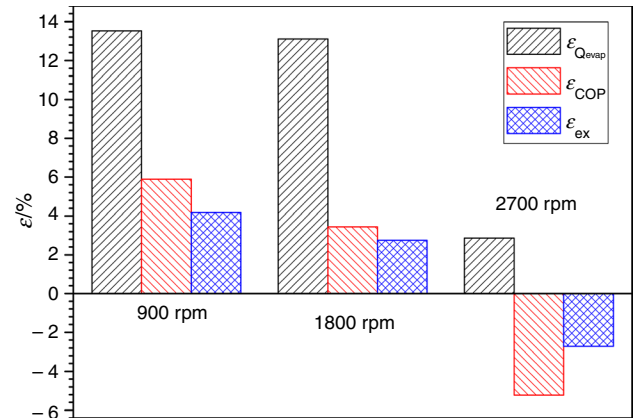

Fig. 12 Difference in cooling capacity, COP and exergy efficiency of the tuned HFO-1234yf with the HFC-134 system with SLHX

cooling capacity is found to be 5.3%, 8.5% and 5.2% at 900, 1800 and 2700 rpm, respectively, with the rise in COP by 2.1%, 4.6% and 3.8%. Similarly, the exergy efficiency of the HFO-1234yf system is increased by 2%, 2.87% and 2.57% for compressor speed of 900, 1800 and 2700 rpm, respectively. The compressor power consumption also increases by 3.1%, 3.7%, and 1.4%, respectively, for the three speeds. The increase in exergy efficiency and COP of the HFO-1234yf system with tuned TXV is not significant like cooling capacity, which is mainly due to the increase in compressor power consumption because of the increased HFO-1234yf mass
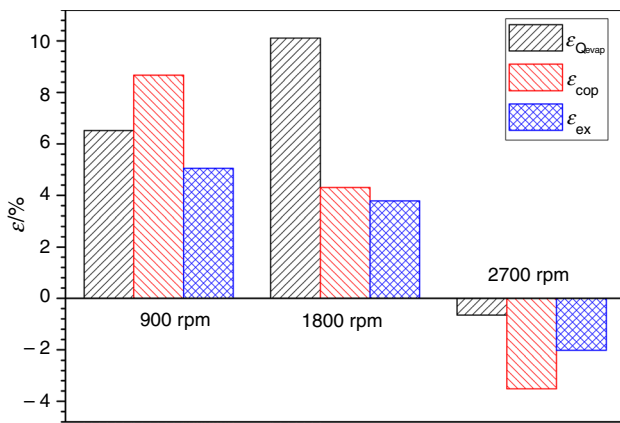
Fig. 13 Difference in cooling capacity, COP and exergy efficiency of the tuned HFO-1234yf system with the baseline system

flow rate. Junye et al. [18] also reported similar results that the MAC system retrofitted with HFO-1234yf had 13% and

$$\text{Indirect emission} = \left(\frac{M_\text{f}}{10,000} \times \frac{\text{km year}}{+} \frac{M_\text{f} \times M_\text{s}}{10,000 \times 100} \times \frac{\text{km}}{\text{year}} \right) \times \frac{\text{COP}_\text{ref}}{\text{COP}_\text{alt}} \times \beta \tag{23}$$

8% improved cooling capacity and COP, respectively, with optimised TXV.

The difference in cooling capacity, COP and exergy efficiency between the tuned HFO-1234yf system and HFC-134a system with SLHX is shown in Fig. 12. It shows that the tuned HFO-1234yf system performance is superior to that of HFC-134a system in terms of cooling capacity, COP and exergy efficiency at idle and city speed conditions. The TXV tuning has enhanced the performance of HFO-1234yf at city limit speed. This increases the cooling capacity and COP by 13.1% and 3.4%, respectively. The existing HFC-134a system still has better COP and exergy efficiency than that of the tuned HFO-1234yf system at high speed. Nevertheless, the cooling capacity of the tuned system is 2.87% higher because of the higher HFO-1234yf mass flow realised.

Similarly, energy and exergy performance difference between the tuned HFO-1234yf system and the existing HFC-134a system [29] is shown in Fig. 13. It shows that the cooling capacity, COP, and exergy efficiency of the tuned HFO system at idle and city speed conditions are increased by 6.5–10.1%, 4.3–8.6% and 3.7–5.1%, respectively, than that of the existing system. However, the existing system still has better performance than that of the tuned HFO-1234yf system at high speed. The TXV tuning has a positive impact on the performance of HFO-1234yf system with SLHX at the considered conditions. From this study, it is inferred that the TXV tuning in the HFO-12343yf system with SLHX

has superior performance than that of the existing HFC-134a system at low speeds and slightly poorer at high-speed conditions.

TEWI analysis

The TEWI analysis was used to estimate the overall global warming effects due to the air conditioning system operation. It can be divided into two categories namely (1) effects due to the refrigerant loss from the unit (Direct emission) and (2) the CO_2 emission from the fossil fuel burnt (indirect emission) to generate the power that is used to run the air conditioning unit [32]. The TEWI can be calculated by using the following equation [33],

$$\text{TEWI} = \text{Direct emission} + \text{Indirect emission} \tag{21}$$

$$\text{Direct emission} = \left(\text{GWP} \times L \times N \times M_\text{s} \right) + \left(\text{GWP} \times M_\text{s} \times (1 - \alpha) \right) \tag{22}$$

In the above equations, L is the average refrigerant leakage from the MAC system per year (20%) [33]; N is the system lifetime (15 years); M_s is the refrigerant charge quantity; α is the percentage of refrigerant recovered from the system (70%); M_f is the fuel consumed due to AC compressor operation; β is the Carbon-dioxide emission factor. The parameters of the midsize passenger car for calculating the TEWI are shown in Table 6.

The TEWI results for the existing HFC-134a system, HFC-134a with SLHX, HFO-1234yf with SLHX systems and tuned HFO-1234yf system with SLHX are shown in Table 7. It shows that the direct emission of the MAC system with HFO-1234yf is almost negligible (lower by 99.7%) in comparison with the existing HFC-134a because of its very low GWP of 4. The total equivalent CO_2 emission of HFO-1234yf system with SLHX and tuned HFO-1234yf system

Table 6 Parameters of the midsize passenger car [33]

Parameters	Values
Mileage without air conditioning/km L^{-1}	18.3
Mileage with air conditioning/km L^{-1}	16.4
Fuel density/kg m^{-3}	750
CO_2 emissions/kg of CO_2 L^{-1}	2.31
CO_2 emissions/kg of CO_2 km^{-1}	0.1408

Table 7 TEWI results

Life time Emission/kg of CO_2-eq	Baseline HFC-134a	HFC-134a with SLHX	HFO-1234yf with SLHX	Tuned HFO-1234yf with SLHX
Direct	2925.78	3492.06	8.844	8.844
Indirect	8810.49	8734.18	8835.51	8443.52
Total	11736.27	12226.24	8844.36	8452.36

are found to be 24.64% and 27.98% lower than those of the existing HFC-134 system.

Conclusions

The effect of TXV tuning on the performance enhancement and environmental impact of the MAC system with SLHX using HFO-1234yf as an alternative to HFC-134a was carried out experimentally. The influences of compressor speed on the system performance and exergy efficiency were also studied. Based on this study, the following conclusions are made,

- The optimum charge of the HFO-1234yf system was found to be 670 g, which was 9.45% lower than that of the HFC-134a system.
- The COP and exergy efficiency of HFO-1234yf system was 3.71% and 2.57% higher than that of the HFC-134a system at 900 rpm.
- The exergy loss in the compressor, evaporator, and TXV of HFO-1234yf system was higher than those of HFC-134a system by 4.38%, 28.51%, and 115.17%, respectively.
- The TXV tuning had a positive impact on the HFO-1234yf system performance to the extent of 8.5%, 4.6%, and 2.87% improvement in cooling capacity, COP and exergy efficiency.
- The tuned HFO-1234yf system had 13.1% higher cooling capacity and 3.5% higher COP at 1800 rpm compared to the HFC-134a system with SLHX.
- At 2700 rpm, even though the cooling capacity was 2.9% higher, the COP was 5.22% dropped compared to the HFC-134a system with SLHX.
- When compared to the existing HFC-134a system, tuned HFO-1234yf system with SLHX has superior performance at low speeds and slightly poorer at high-speed conditions.
- The TEWI analysis showed that the total CO_2 equivalent emission of tuned and un-tuned HFO-1234yf system was 27.98% and 24.64% lower than that of the existing HFC-134a system.

This study highlights the performance comparison between HFO-1234yf and the existing HFC-134a in a MAC system. It also reports the exergy destruction experienced in each component of the system. Finally the impact of MAC system on the environment also evaluated. It is also concluded that the HFC-134a MAC system can be successfully retrofitted with HFO-1234yf possibly with SLHX and suitable tuning of the TXV.

References

1. Dutt GS. Energy-efficient and environment-friendly refrigerators. Int Energy Sustain Dev. 1995;1(5):57–68. https://doi.org/10.1016/S0973-0826(08)60089-7.
2. UNEP. The Kigali amendment to the montreal protocol: HFC phase-down. In: 28th meeting of parties to Montreal protocol. 2016, Kigali, Rwanda.
3. Directive 2006/40/EC of the European parliament and of the council of 17 May relating to emissions from air conditioning systems in motor vehicles and amending council directive 70/156/EEC. Official Journal of the European Union. 2006;161:12–18. https://eur-lex.europa.eu/LexUriServ/LexUriServ.do?uri=OJ:L:2006:161:0012:0018:EN:PDF.
4. Lambert MA, Jones BJ. Automotive adsorption air conditioner powered by automotive exhaust, part 1: conceptual and embodiment design. Proc Inst Mech Eng Part D J Automob Eng. 2006;220(7):959–72. https://doi.org/10.1243/09544070JAUTO221.
5. Mohanraj M. Energy performance assessment of R430A as a possible alternative refrigerant to R134a in domestic refrigerators. Energy Sustain Dev. 2013;17:471–6. https://doi.org/10.1016/j.esd.2013.05.005.
6. Sanchez D, Cabello R, Llopis R, Arauzo I, Catalan-Gil J, Torrella E. Energy performance evaluation of R1234yf, R1234ze(E), R600a, R290 and R152a as low-GWP R134a alternatives. Int J Refrig. 2017;74:269–82. https://doi.org/10.1016/j.ijrefrig.2016.09.020.
7. Tanaka K, Higashi Y. Thermodynamic property modelling for 2,3,3,3-tetrafluoropene (R-1234yf). Int J Refrig. 2010;33:52–60. https://doi.org/10.1016/j.ijrefrig.2009.10.003.
8. ANSI/ASHRAE Standard 34. Designation and safety classification of refrigerants. 2013. ISSN:1041-2336. https://www.ashrae.org/File%20Library/Technical%20Resources/Standards%20and

%20Guidelines/Standards%20Addenda/34_2013_2015Supplement_20150210.pdf.

9. Nielsen OJ, Javadi MS, Andersen MPS, Hurley MD, Wallington TJ, Singh R. Atmospheric chemistry of $CF_3CF=CH_2$: Kinetics and mechanisms of gas-phase reactions with Cl atoms, OH radicals, and O_3'. Chem Phys Lett. 2007;439:18–22. https://doi.org/10.1016/j.cplett.2007.03.053.

10. Lueken DJ, Waterland RT, Papasavva S, Taddonio KN, Hutzell WT, Rugh JP, Andersen SO. Ozone and TFA impacts in North America from degradation of 2,3,3,3-tetrafluoropropene (HFO-1234yf), a potential greenhouse gas replacement. Environ Sci Technol. 2010;44:343–8. https://doi.org/10.1021/es902481f.

11. Kajihara H. Estimation of environmental concentrations and deposition fluxes of R-1234yf and its decomposition products emitted from air conditioning equipment to atmosphere. In: International symposium on next-generation air conditioning and refrigeration technology, Tokyo, 2010.

12. Lewandowski TA. Additional risk assessments of alternative refrigerant R1234yf. SAE International CRP1234-4 report, 2013.

13. Environmental Protection Agency (EPA). protection of stratospheric ozone: change of listing status for certain substitutes under the significant new alternatives policy program; final rule. Federal register, rules and regulations 2015; 80(138): July 20.

14. Jarall S. Study of refrigeration system with HFO-1234yf as a working fluid. Int J Refrig. 2012;35:1668–77. https://doi.org/10.1016/j.ijrefrig.2012.03.007.

15. Mota-Babiloni A, Navarro-Esbri J, Barragan-Cervera A, Moles F, Peris B. Drop-in energy performance evaluation of R1234yf and R1234ze(E) in a vapour compression system as R134a replacements. Appl Therm Eng. 2014;71:259–65. https://doi.org/10.1016/j.applthermaleng.2014.06.056.

16. Lee Y, Jung D. A brief performance comparison of R1234yf and R134a in a bench tester for automobile applications. Appl Therm Eng. 2012;35:240–2. https://doi.org/10.1016/j.applthermaleng.2011.09.004.

17. Sukri MF, Musa MN, Senawi MY, Nasution H. Achieving a better energy-efficient automotive air-conditioning system: a review of potential technologies and strategies for vapour compression refrigeration cycle. Energy Eff. 2015;8:1201–29. https://doi.org/10.1007/s12053-015-9389-4.

18. Junye S, Cichhong L, Jichao H, Yu Z, Jiangping C. Experimental research and optimization on the environmental friendly R1234yf refrigerant in automobile air conditioning system. J Shanghai Jiaotong Univ (Sci.). 2016;21(5):548–56. https://doi.org/10.1007/s12204-016-1761-9.

19. Zilio C, Brown JS, Schiochet G, Cavallini A. The refrigerant R1234yf in air conditioning systems. Energy. 2011;36:6110–20. https://doi.org/10.1016/j.energy.2011.08.002.

20. Rajendran P, Dhasan ML, Narayanaswamy GR. Tuning thermostatic expansion valve for implementing suction line heat exchanger in mobile air conditioning system. J Braz Soc Mech Sci Eng. 2019;41:191. https://doi.org/10.1007/s40430-019-1680-4.

21. Devecioglu AG, Oruc V. Improvement on the energy performance of a refrigeration system adapting a plate-type heat exchanger and low-GWP refrigerants as alternatives to R134a. Energy. 2018;155:105–16. https://doi.org/10.1016/j.energy.2018.05.032.

22. Desai AD, Sapli SN, Garikipati PV. Development of energy efficient R-134a automotive air conditioning system using internal heat exchanger. International proceedings of the world congress on engineering, Vol. III, July 6–8, 2011, London, U.K. https://pdfs.semanticscholar.org/c077/f5d5b1f6f1df0eaf6d713171e64cff00b3c6.pdf.

23. Navarro-Esbri J, Moles F, Barragan-Cervera A. Experimental analysis of the internal heat exchanger influence on a vapour compression system performance working with R1234yf as a drop-in

replacement for R134a. Appl Therm Eng. 2013;59:153–61. https://doi.org/10.1016/j.applthermaleng.2013.05.028.

24. Cho H, Lee H, Park C. Performance characteristics of an automobile air conditioning system with internal heat exchanger using refrigerant R1234yf. Appl Therm Eng. 2013;61:563–9. https://doi.org/10.1016/j.applthermaleng.2013.08.030.

25. Kurata S, Suzuki T, Ogura K. Double-pipe internal heat exchanger for efficiency improvement in front automotive air conditioning system. 2007. SAE Technical Paper 2007-01-1523. https://doi.org/10.4271/2007-01-1523.

26. Qi Z, Zhao Y, Chen J. Performance enhancement study of mobile air conditioning system using microchannel heat exchanger. Int J Refrig. 2010;33:301–12. https://doi.org/10.1016/j.ijrefrig.2009.08.014.

27. Cho H, Park C. Experimental investigation of performance and exergy analysis of automotive air conditioning systems using refrigerant R1234yf at various compressor speeds. Appl Therm Eng. 2016;101:30–7. https://doi.org/10.1016/j.applthermaleng.2016.01.153.

28. Paradeshi L, Mohanraj M, Srinivas M, Jayaraj S. Exergy analysis of direct-expansion solar-assisted heat pumps working with R22 and R433A. J Therm Anal Calorim. 2018;134:2223–37. https://doi.org/10.1007/s10973-018-7424-3.

29. Prabakaran R, Lal DM. A novel exergy based charge optimisation for a mobile air conditioning system—an experimental study. J Therm Anal Calorim. 2018;132:1241–52. https://doi.org/10.1007/s10973-018-6998-0.

30. Golzari S, Kasaeian A, Daviran S, Mahian O, Wongwises S, Sahin AZ. Second law analysis of an automotive air conditioning system using HFO-1234yf, an environmentally friendly refrigerant. Int J Refrig. 2017;73:134–43. https://doi.org/10.1016/j.ijrefrig.2016.09.009.

31. Wu X, Hu S, Mo S. Carbon footprint model for evaluating the global warming impact of food transport refrigeration systems. J Clean Prod. 2013;54:115–24. https://doi.org/10.1016/j.jclepro.2013.04.045.

32. Papasavvaa S, Andersen SO. GREEN-MAC-LCCP: life-cycle climate performance metric for mobile air conditioning technology choice. Environ Prog Sustain Energy. 2011;30(2):234–47. https://doi.org/10.1002/ep.10465.

33. Abraham JAP, Mohanraj M. Thermodynamic performance of automobile air conditioners working with R430A as a drop-in substitute to R134a. J Therm Anal Calorim. 2018;136(5):2071–86. https://doi.org/10.1007/s10973-018-7843-1.

34. Mastrullo R, Mauro AW, Vellucci C. Refrigerant alternatives for high speed train A/C systems: energy savings and environmental emissions evaluation under variable ambient conditions. Energy Proc. 2016;101:280–7. https://doi.org/10.1016/j.egypro.2016.11.036.

35. Aprea C, Greco A, Maiorino A. An experimental evaluation of the greenhouse effect in the substitution of R134a with CO_2. Energy. 2012;45:753–61. https://doi.org/10.1016/j.energy.2012.07.015.

36. SAE J 2765. Procedure for measuring system COP (Coefficient of Performance) of a mobile air conditioning system on a test bench; 2008. https://saemobilus.sae.org/content/j2765_200810.

37. Prabakaran R, Lal DM, Prabhakaran A, Kumar JK. Experimental investigations on the performance enhancement using minichannel evaporator with integrated receiver-dryer condenser in an automotive air conditioning system. Heat Transf Eng. 2019;40(8):667–78. https://doi.org/10.1080/01457632.2018.1436663.

38. Rajendran P, Sidney S, Ramakrishnan I, Dhasan ML. Experimental studies on the performance of mobile air conditioning system using environmental friendly HFO-1234yf as a refrigerant. Proc Inst Mech Eng Part E J Process Mech Eng. 2019. https://doi.org/10.1177/0954408919881236.

39. Dincer I, Kanoglu M. Refrigeration systems and applications. 2nd ed. New York: Wiley; 2010.

40. Lemmon EW, Huber ML, McLinden MO. Reference fluid thermo-dynamic and transport (REFPROP). Version 8.0, NIST standard database 23, 2007. National Institute of Standard and technology, Gaithersburg, MD, USA.

41. Moffat RJ. Describing the uncertainties in experimental results. Exp Thermal Fluid Sci. 1988;1:3–17. https://doi.org/10.1016/0894-1777(88)90043-X.

42. Zhao Y, Qi Z, Chen J, Xu B, He B. Experimental analysis of the low—GWP refrigerant R1234yf as a drop-in replacement for R134a in a typical mobile air conditioning system. Proc Mech Eng Part C J Mech Eng Sci. 2012;226:2713–25. https://doi.org/10.1177/0954406211435583.